

Polymer Lung Surfactants

Hyun Chang Kim,[†] Madathilparambil V. Suresh,[‡] Vikas V. Singh,[‡] Davis Q. Arick,[†]
David A. Machado-Aranda,[‡] Krishnan Raghavendran,[‡] and You-Yeon Won^{*,†}

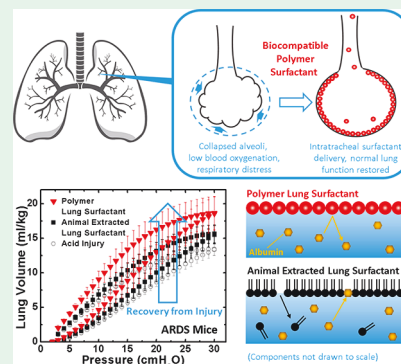
[†]Davidson School of Chemical Engineering, Purdue University, West Lafayette, Indiana 47907, United States

[‡]Department of Surgery, University of Michigan, Ann Arbor, Michigan 48109, United States

Supporting Information

ABSTRACT: Animal-derived lung surfactants annually save 40 000 infants with neonatal respiratory distress syndrome (NRDS) in the United States. Lung surfactants have further potential for treating about 190 000 adult patients with acute respiratory distress syndrome (ARDS) each year. To this end, the properties of current therapeutics need to be modified. Although the limitations of current therapeutics have been recognized since the 1990s, there has been little improvement. To address this gap, our laboratory has been exploring a radically different approach in which, instead of lipids, proteins, or peptides, synthetic polymers are used as the active ingredient. This endeavor has led to an identification of a promising polymer-based lung surfactant candidate, poly(styrene-*b*-ethylene glycol) (PS-PEG) polymer nanomicelles. PS-PEG micelles produce extremely low surface tension under high compression because PS-PEG micelles have a strong affinity to the air–water interface. NMR measurements support that PS-PEG micelles are less hydrated than ordinary polymer micelles. Studies using mouse models of acid aspiration confirm that PS-PEG lung surfactant is safe and efficacious.

KEYWORDS: block copolymer micelle, lung surfactant, pulmonary surfactant, acute respiratory distress syndrome, neonatal respiratory distress syndrome



1. INTRODUCTION

The development of therapeutic lung surfactants (LSs), extracted from bovine or porcine lungs, has greatly contributed to reducing the mortality rates of neonatal respiratory distress syndrome (NRDS). NRDS is a complication with a prevalence in the United States of 40 000 cases per year that occurs in preterm infants due to their underdeveloped respiratory system.¹ When infants are born before the full 40 week gestation period, they have a deficiency in LSs.^{2,3} Without LSs, the lung alveoli collapse disproportionately, resulting in a life-threatening situation. Before 1980s, when NRDS was misnamed as “hyaline membrane disease” due to the misconception that this disease was of viral origin, it was the leading cause of infant death in the United States and had a higher death rate than pneumonia or influenza.^{4,5} With the discovery of the LS’s pivotal role in the lung mechanics, treatments involving instillation of therapeutic LSs to NRDS infants have reduced the NRDS-related mortality rates to 2%.⁶

LS complication can also occur in adults and pediatrics. The most-severe form of respiratory failure is termed acute respiratory distress syndrome (ARDS).³ ARDS is a physiological syndrome that involves multiple risk factors such as sepsis, pneumonia, aspiration-induced lung injury, lung contusion, and massive transfusion. The annual U.S. prevalence of ARDS is 190 000, and despite modern critical care, the mortality rate is ~40%.^{7–10} Regardless of the origin, ARDS patients exhibit increased protein-rich exudates and

inflammation in the alveoli, which result in inactivation and reduced production of lung surfactant. With the success in treatment of NRDS infants with therapeutic LSs, a number of clinical trials investigated their efficacy in treating ARDS patients. Unfortunately, the results from large-scale clinical trials have indicated that current therapeutic LSs are not effective in treating adult ARDS.^{11–14} However, there were two critical issues with previous clinical trials. (1) Current therapeutic LSs are not designed to be resistant to deactivation caused by serum proteins.^{12,15,16} (2) The LS dose levels used were inappropriate.^{17,18} Both of these factors are related to the mechanism of LS’s surface activity.

Although therapeutic LSs from animal sources and endogenous human LSs are different slightly in composition, they both overall contain about 90% lipids (mainly phospholipids plus cholesterol) and 10% surfactant proteins.³ The phospholipids reside at the air–water interface and lower the air–water interfacial tension proportionally to the radius of the alveolus (and, thus, to the square root of the surface area of the alveolus). The size-dependent reduction of the air–water interfacial tension consequently equalizes the Laplace pressure (ΔP) between differently sized alveoli, as shown in Figure 1a. The air–water interfacial mechanical properties of LSs are

Received: May 3, 2018

Accepted: August 22, 2018

Published: August 22, 2018

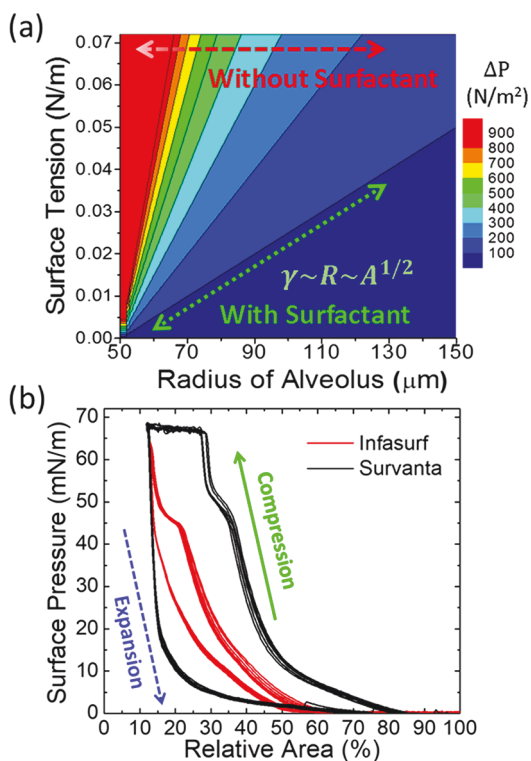


Figure 1. (a) Contour plot of the Laplace pressure (ΔP) of a spherical alveolus calculated as a function of surface tension (γ) and radius (R). (b) Surface pressure vs relative area isotherms of Infasurf and Survanta obtained during repeated continuous compression–expansion cycles. The data displayed represent the last 10 compression–expansion cycles of total 50 continuous cycles. The subphase solution used contained 150 mM NaCl, 2 mM CaCl_2 , and 0.2 mM NaHCO_3 (pH 7.0–7.4, 25 °C). The monolayer was compressed and expanded at a rate of 50 mm/min; one compression–expansion cycle took 7.18 min. At the “100% relative area”, 10 mg of Infasurf and Survanta was spread on water in a Langmuir trough with a 780 cm^2 surface area and a 1.4 L subphase volume; “100% relative areas” corresponded to 0.972 square angstroms per molecule for both Infasurf and Survanta.

typically studied by measurements of surface pressure versus area isotherms during compression–expansion cycles. The surface pressure–relative area isotherms for two commercial therapeutic surfactants, Infasurf (ONY, calf lung lavage) and Survanta (AbbVie, bovine lung mince), are shown in Figure 1b; detailed composition information for these commercial LS products has been summarized in a recent review article.¹⁹ Here, the surface pressure (π) is defined as the difference between the surface tension of the clean air–water interface (γ_0) and that of the LS-laden air–water interface (γ); that is, $\pi = \gamma_0 - \gamma$. For both Infasurf and Survanta, a sharp increase in surface pressure (sharp decrease in surface tension) was observed upon compression, while a sharp decrease in surface pressure (sharp increase in surface tension) was seen upon expansion.

During compression–expansion cycles, phospholipids desorb from the air–water interface at high compression and readsorb to the air–water interface upon expansion (with the aid of surfactant proteins such as SP-B and SP-C).^{20,21} It is this desorption–readsorption mechanism that makes lipid- and protein-based LSs susceptible to deactivation and complicates dose estimation for ARDS treatment. Typically the lungs of an ARDS patient are flooded with fluids rich in albumin,

fibrinogen, and hemoglobin (collectively referred to as “deactivating agents”).^{3,22–25} These deactivating agents have a higher tendency to adsorb to the air–water interface than LS lipids.^{24–26} Thus, after a few breathing cycles, LSs at the air–water interface are replaced by these deactivating proteins; see the lower right panel of the Table of Contents graphic. In previous ARDS clinical trials, high doses of therapeutic LSs have typically been used with the hope that the excess amount of LSs leads to a re-replacement of the deactivating agents at the air–water interface by the therapeutic surfactants.²⁶ However, clinical data suggest that this is not an effective strategy.^{11–14} We propose an alternative method for ARDS treatment: the use of therapeutic surfactants that are resistant to deactivation by proteins (as depicted in the lower right panel of the Table of Contents graphic). All currently available lipid- and protein-based LSs fall short in this regard. The use of polymers as additives to suppress the serum inactivation of lipid- and protein-based LSs^{24,25} or as a surrogate for SP-B proteins²³ has previously been proposed. However, to our knowledge, using polymers as a main active ingredient for surfactant replacement therapy is a new concept that has never before been explored.

The desorption–readsorption mechanism also poses a problem in estimating the optimal dose. If the same dosing strategy for therapeutic LSs is used in adult ARDS patients as that used in NRDS infants, the recommended dose is 100 mg of phospholipids per kilogram of body weight; in terms of injection volume, the number becomes 3–4 mL of LS suspension per kilogram of body weight. The “100 mg/kg” dose represents an amount that is about 32 times in excess of that needed to fully coat the whole surface area of the lungs of an infant (3.1 mg/kg).²⁷ The use of excess LSs is necessary because the aqueous subphase of the alveolar air–water interface (alveolar lining fluid) needs to be saturated with LSs to guarantee the proper operation of the surfactant adsorption–desorption process.³ The lungs of infants have less branching than those of adults, and therefore, the above simple volumetric scaling is inadequate when applied to adult ARDS patients, for instance, due to wall losses of liquids during bolus delivery (“coating cost”).¹⁷ Furthermore, an instillation of 3–4 mL/kg of liquid to an adult ARDS patient is inadequate because the patient’s lungs are already filled with fluid. Unfortunately, clinical trials testing lower volumetric doses were unsuccessful.^{11–13} A recent study suggested that, despite the coating cost, the 4 mL/kg dose delivers sufficient surfactant material to the alveoli of an adult ARDS patient.^{17,18}

A potential solution to this conundrum is aerosol delivery. However, efforts to aerosolize therapeutic LS have only met with technical difficulties.²⁸ Liquid foaming is, for instance, one challenge; the typical concentration of active ingredient in a commercial LS preparation is about 25 mg/mL (Survanta), which has a high viscosity and a low surface tension and is thus prone to foaming and swelling.¹⁹ Even with advancement of the nebulization technology, producing a steady stream of aerosolized LS at a high dose of 100 mg/kg without clogging the nebulization device remains challenging.²⁹

A solution to both the deactivation and high-dose problems is to develop a material that can function as LS by a completely different mechanism, i.e., via the formation of an insoluble monolayer at the air–water interface. Such a compound, being insoluble, would have a higher affinity to the air–water interface than serum proteins and thus be resistant to deactivating effects of serum proteins because it does not

desorb from the air–water interface. Also, a much-lower dose would be required of such compound (estimated to be 3.1 mg/kg) relative to current therapeutic LSs (100 mg/kg). With polymer formulations, aerosolization would be easier, too, because lower concentrations can be used. For these reasons, we think that polymers are ideal materials to be used as active ingredients in ARDS therapeutics. Polymer LSs are free of pathogenic contaminants. The most-important advantage of synthetic polymer LSs over animal-derived products is mass production. If surfactant-replacement therapy becomes the standard of care for ARDS treatment, the increase in demand for therapeutic LSs cannot be met by the current manufacturing method (extraction of lipid and protein active ingredients from bovine and porcine lungs).¹⁹ High-quality polymer LSs can easily be mass-produced at lower costs. From our study over the past several years, we have developed design criteria for polymer LSs; a successful LS candidate should (1) be biocompatible and biodegradable, (2) produce an extremely low surface tension at high compression ($\ll 10$ mN/m) repeatedly during multiple compression–expansion cycles, (3) be resistant to serum proteins, and (4) (in the end) prove to be safe and effective in preclinical (animal) models. A wide range of polymers have been searched and tested; for instance, see refs 30–32. Recently, we have identified a promising class of candidate materials: polymer micelles having highly hydrophobic cores (such as those formed by poly(styrene-*block*-ethylene glycol) (PS–PEG) block copolymers). These materials meet all the performance criteria stated above, and additionally, these materials can easily be formulated in aqueous injectable dosage forms. The treatment safety and efficacy of PS–PEG micelles have been validated in ARDS mouse models. While this finding is a significant step toward developing alternative surfactant therapeutics, it had also brought important scientific questions concerning mechanisms by which these materials produce extremely low surface tension at high compression. Answering these questions has also been an important part of this study. The present paper details extensive work involved in the rational design and development of polymer lung therapeutics.

2. EXPERIMENTAL PROCEDURES

PLGA–PEG Synthesis. The PLGA–PEG material used was synthesized by ring-opening polymerization using a tin catalyst. Purified poly(ethylene glycol) monomethyl ether (PEG–OH; number-average molecular weight, M_n , of 5000 g/mol, Sigma-Aldrich) was used as the macroinitiator, and tin(II) 2-ethylhexanoate (Sigma-Aldrich) was used as the catalyst. The polymerization reactions were run at 130 °C. The D,L-lactide (Lactel) and glycolide (Sigma-Aldrich) monomers were twice recrystallized from toluene (Sigma-Aldrich) and tetrahydrofuran (Sigma Aldrich) prior to use. The synthesized PLGA–PEG product was precipitated in 2-propanol (Sigma-Aldrich) and dried under a vacuum before use and storage at refrigeration temperatures.

PS–PEG Synthesis. PS–PEG materials were synthesized by reversible addition–fragmentation chain-transfer (RAFT) polymerization. 4-Cyano-4-[(dodecylsulfanyliothiocarbonyl)sulfanyl] pentanoic acid (Sigma-Aldrich) was used as the RAFT agent. First, the RAFT agent was conjugated to purified poly(ethylene glycol) monomethyl ether (PEG–OH, M_n = 5000 g/mol, Sigma-Aldrich) by Steglich esterification.³³ The PEG–OH (1 g, 0.2 mmol), the RAFT agent (161.4 mg, 0.4 mmol), and 4-dimethylaminopyridine (Sigma-Aldrich, 4.89 mg, 0.04 mmol) were mixed in 10 mL dichloromethane (Sigma-Aldrich) and kept under magnetic stirring at 0 °C. A separately prepared dicyclohexylcarbodiimide (82.5 mg, 0.4 mmol) solution in dichloromethane (5 mL) was drop-wise added to the above mixture

and was allowed to undergo reaction for 5 min at 0 °C and then for 3 h at 20 °C to produce “PEG–RAFT”. The as-synthesized PEG–RAFT product was first filtered through filter paper to remove the insoluble urea byproduct and was then further purified by precipitation in hexane twice. The RAFT polymerization reaction was performed at 70 °C by mixing the PEG–RAFT, inhibitor-free styrene (Sigma-Aldrich), and a free radical initiator, azobis(isobutyronitrile) (Sigma-Aldrich) in dioxane (Sigma-Aldrich). The resulting PS–PEG products were precipitated twice in hexane and dried under vacuum.

Polymer Characterizations. The number-average molecular weights of the polymers were determined by ¹H nuclear magnetic resonance (NMR) spectroscopy using a Bruker ARX NMR spectrometer (500 MHz). For ¹H NMR measurements, polymer samples were prepared in deuterated chloroform at a polymer concentration of 5 wt %. The polydispersity indices (PDIs) of the polymers were measured by size-exclusion chromatography (SEC) using an Agilent Technologies 12000 Series instrument equipped with a Hewlett-Packard G1362A refractive index detector and 3 PLgel 5 μ m MIXED-C columns. Tetrahydrofuran was used as the mobile phase (kept at 35 °C, flowing at a rate of 1 mL/min). Calibration was performed using polystyrene standards (Agilent Easi Cal).

Surface-Pressure–Area Isotherms. The surface tension–area isotherms for Infasurf, Survanta, and polymer LSs were measured using a KSV 5000 Langmuir trough (51 cm \times 15 cm) with double symmetric barriers. The total surface area of the trough was 780 cm², and the subphase volume was 1.4 L. A filter paper Wilhemly probe was used for surface tension measurements. Before each measurement run, the trough and the barriers were cleaned three times using ethanol and Milli-Q-purified water. The surface of water was also aspirated to remove any surface active contaminants. When the water surface was completely clean, the surface tension reading did not change during a blank compression run. LS samples were spread onto water using a Hamilton microsyringe, i.e., by forming a microliter-sized droplet at the tip of the syringe needle and letting it contact the water surface. The Langmuir trough was used to create a system that mimics the air–water interface of the alveolus. However, it should be noted that only qualitative connections can be established between the actual breathing process (e.g., Figure 1a) and the Langmuir trough experiment (Figure 1b) because of the differences in such parameters as the compression and expansion rate, surface area to volume ratio, interfacial curvature, etc.

Polymer Micelle Preparation. The solvent-exchange procedure was used to prepare spherical polymer micelles. A total of 200 mg of the polymer was first dissolved in 4 mL of acetone (Sigma-Aldrich). Then, 36 mL of Milli-Q-purified water (18 M Ω ·cm resistivity) was drop-wise added to the polymer solution at a rate of 0.05 mL/min using a syringe pump, and the mixture was kept under vigorous stirring for 24 h. To remove the acetone, the solution was transferred to a dialysis bag (Spectra/Por 7, 50 kDa molecular weight cutoff) and dialyzed for 3 h against 1 L of Milli-Q-purified water. The reservoir was replaced with fresh Milli-Q water every hour.

Polymer Micelle Characterizations. The hydrodynamic diameters of the block copolymer micelles were measured at 25 °C by dynamic light scattering (DLS) using a Brookhaven ZetaPALS instrument. The scattering intensities were measured using a 659 nm laser at a scattering angle of 90 °. The hydrodynamic diameters were calculated from the measured diffusion coefficients using the Stokes–Einstein equation. For DLS measurements, the samples were diluted to guarantee single scattering and were filtered with 0.2 μ m syringe filters to remove contaminants.

Transmission electron microscopy (TEM) was used to image the polymer micelles. TEM specimens were prepared by placing 20 μ L of a 0.01–0.05 mg/mL polymer micelle solution on a carbon-coated copper TEM grid (hydrophobically treated using a O₂ plasma cleaner). A total of 10 μ L of a 2% uranyl acetate solution was added to the sample solution already placed on the TEM grid, and the mixture was blotted using filter paper and dried. The samples thus prepared were imaged using a 200 kV FEI Tecnai 20 TEM instrument. The

TEM images were analyzed using the Gatan Digital Micrograph software.

NMR Spin-Relaxation Measurements. NMR spin relaxation measurements were performed using a Bruker Avance-III-800 Spectrometer equipped with a sample temperature-control unit. PLGA-PEG and PS-PEG micelle samples were prepared using the solvent exchange procedure (described above) using D₂O (instead of H₂O) as the final solvent. The PEG homopolymer sample was prepared by directly dissolving PEG in D₂O. In all samples, the polymer concentration was 0.5 wt %. The inversion recovery sequence was used for T_1 relaxation measurements, and the Carr–Purcell–Meiboom–Gill (CPMG) pulse sequence was used for T_2 relaxation measurements. Data were fit to single or bi-exponential decay functions using the nonlinear least-squares regression technique.

Evaluation of the Tolerability of Intratracheally Injected Polymer LSs in Adult Mice. In this study, C57/BL6 mice (8–12 weeks old, female) were used. Prior to intratracheal instillation of polymer LSs, mice were anesthetized using isoflurane. Mice were then placed on a custom-designed angled platform with its incisors hung on a wire. The tongue was pulled out of the mouse using forceps, and 4 milliliters of polymer LS solutions per kilogram of body weight containing different concentrations of polymers were directly dropped into the opening of the trachea using a micropipette. Mice were left to naturally recover from anesthesia.

For the MTD evaluation, mice were intratracheally instilled with 3 different doses of PS(4418)–PEG(5000) micelles (2.4, 24, and 240 mg/kg) and examined for 2 weeks for symptoms of toxicity (weight loss, activity level, etc.). After day 14, mice were humanely sacrificed.

For bronchoalveolar lavage (BAL) fluid and histology analysis, mice were sacrificed at day 7 following the intratracheal instillation of 240 mg PS(4418)–PEG(5000) micelles per kilogram of body weight. BAL fluids were collected by injecting and recovering a pair of 0.6 mL aliquots of ice-chilled phosphate-buffered saline. A pair of aliquots were combined and centrifuged at 150g and 4 °C for 10 min to remove cells and particles. Levels of albumin and four immune makers (IFN- γ , TNF- α , MCP-5, and IL-6 cytokines) in the BAL fluid samples were analyzed using the method described in ref 34.

Closed-Chest Pressure–Volume Analysis of Acid-Injured Mouse Lungs after Treatment with Polymer LSs. C57/BL6 mice (8–12 weeks old, female) were used in this study. Acute lung injury was produced by intratracheal installation of 30 μ L of 0.25 N HCl using the procedure described above. At 5 h after acid aspiration, mice were intratracheally instilled with 3 mL/kg of Infasurf (35 mg/mL), 4 mL/kg of PS(4418)–PEG(5000) micelles (0.6, 6, or 60 mg/mL), or 4 mL/kg of 0.9% saline. At 10 min following LS treatment, mice were sacrificed using excess ketamine. Immediately after sacrifice, the mice trachea was cut open by surgical incision and connected to a Flexivent SCIREQ ventilator through an 18 g blunt-end needle (inserted into the trachea). A prescribed ventilation sequence was executed to obtain closed-chest pressure–volume curves. Details of the ventilation setup and parameters used can be found in ref 34.

Regulatory Compliance Statement. All animal study procedures are in compliance with relevant state and federal regulations and also with the Association for Assessment and Accreditation of Laboratory Animal Care International standards and have been approved by the Institutional Animal Care and Use Committee of the University of Michigan Medical School, Ann Arbor, MI (approval no. PRO00007876).

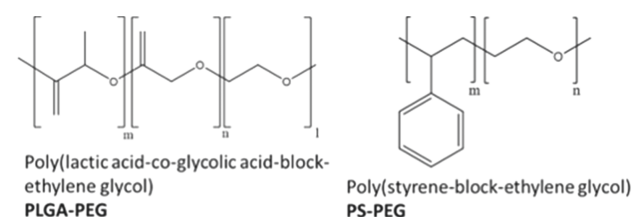
Statistical Analysis of in Vivo Data. The statistical significance of the data presented in Figure 7 was evaluated by one-way analysis of variance using the GraphPad Prism 6.01 software (GraphPad Software Inc., La Jolla, CA). Groups were compared by two-tailed unpaired t test with the Welch's correction. The observed difference is not statistically significant if the p value is greater than 0.05. The p values of individual experiments are summarized in Table S1.

The statistical significance of the data presented in Figure 8 was also similarly analyzed. A one-way analysis of variance (ANOVA) was used to determine whether there was a statistically significant difference in effect between different treatment groups. The results of this analysis (i.e., the p values) are summarized in Table S2.

Significance levels are defined as * ($p < 0.05$), ** ($p < 0.01$), *** ($p < 0.001$), and **** ($p < 0.0001$).

3. RESULTS AND DISCUSSION

Biocompatibility. Biocompatibility is an essential prerequisite for clinical use. For this reason, our investigation has been focused on PEGylated amphiphilic block copolymers. A pair of examples of materials will be discussed in this article; the first is the Food and Drug Administration approved biodegradable block copolymer, poly(lactic acid-*co*-glycolic acid-*block*-ethylene glycol) (PLGA-PEG),^{35–39} and the second is poly(styrene-*block*-ethylene glycol) (PS-PEG) (Figure 2). In their micelles, the hydrophobic PLGA or PS



Polymer	$M_{n,PEG}$ (g/mol)	$M_{n,PLGA/PS}$ (g/mol)	PDI
PLGA(4030)-PEG(5000)	5,000	4,030†	1.41
PS(1560)-PEG(5000)	5,000	1,560	1.10
PS(2993)-PEG(5000)	5,000	2,993	1.13
PS(4418)-PEG(5000)	5,000	4,418	1.34
PS(5610)-PEG(5000)	5,000	5,610	1.16
PS(13832)-PEG(5000)	5,000	13,832	1.38

Figure 2. Molecular characteristics of polymer LS candidate materials investigated in this study. The dagger indicates a ratio of lactic acid to glycolic acid of 47:53 by mole.

chains form micelle core domains, and the hydrophilic PEG chains form micelle coronae. In the literature, PLGA-PEG and PS-PEG micelles have been documented as biosafe.^{35–39}

For this study, monodisperse PLGA-PEG and PS-PEG micelles with well-defined sizes and shapes were prepared using the solvent exchange methodology.^{40,41} Although PLGA-PEG spontaneously degrades in aqueous media over a time scale of months, PS-PEG micelles were permanently stable (stable for years) at room temperature. Also, these polymer micelles did not require any pretreatment processes in order to obtain reproducible effects. Conventional lipid-based LSs typically have short shelf lives (<12 months) and require cold storage (at 2–8 °C) and/or pretreatment procedures (such as agitation and warming of the fluid) before use. This advantage in handling characteristics alone can contribute to effectively reducing the total treatment cost.

Extremely Low Surface Tension (High Surface Pressure) at High Compression. The primary role of LS is to reduce work of breathing (and thus also to prevent atelectrauma) by lowering the alveolar air–water interfacial tension. A wide range of polymers have been searched and tested to identify a candidate polymer LS that produces a sufficiently low surface tension at high compression ($\ll 10$ mN/m). Initially, we focused our study on the FDA-approved PLGA-PEG copolymer. If spread appropriately, PLGA-PEG forms a well-spread film at the air–water interface, commonly referred to as a Langmuir monolayer. A Langmuir trough

device was used to create an *in vitro* lung-mimicking test environment. When a sufficient amount of PLGA–PEG is spread on the air–water interface beyond the full coverage point, the PLGA–PEG polymers form a brush-coated insoluble film, in which the PLGA segments are anchored to the water surface (forming a slightly glassy, insoluble polymer film), and the PEG segments are submerged into the water subphase (forming a brush layer).^{30,31} In the highly compressed state, PLGA–PEG reduces the surface tension of water down to close to zero because of the combined effects of PLGA glass transition and PEG brush repulsion.^{31,42} The morphological and surface mechanical properties of Langmuir PLGA–PEG monolayers under various monolayer compression conditions are discussed in detail in refs 31 and 30.

Figure 3 displays the surface pressure–area isotherms obtained from Langmuir monolayers formed by

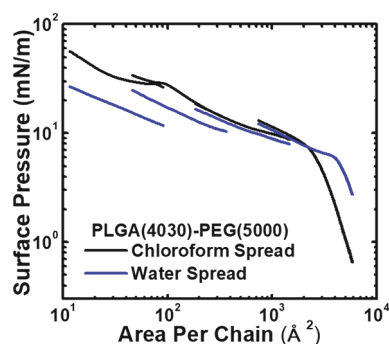


Figure 3. Constant-compression surface pressure–area isotherms of chloroform-spread and water-spread PLGA(4030)–PEG(5000) monolayers on the surface of Milli-Q-purified water (18 M Ω -cm resistivity) at 25 °C. Surface pressure was measured during compression at a rate of 3 mm/min. In the water spread experiments, the mean hydrodynamic diameter of the PLGA–PEG micelles was 75.1 ± 3 nm (measured by DLS). For each solvent group, measurements were performed in four different area ranges because of a small (finite) compression distance of the Langmuir trough to construct an isotherm curve over a full range of area per monomer values; the curves from right to left were obtained, respectively, by initially spreading 4, 16, 64, and 256 μ L of 5 mg/mL PLGA(4030)–PEG(5000) solution (in chloroform or water) on water in a Langmuir trough with a 780 cm² surface area and a 1.4 L subphase volume. Note that the water-spread isotherms obtained in different area ranges do not overlap with each other; this indicates that the water spreading process involves significant loss of polymer to the aqueous subphase.

PLGA(4030)–PEG(5000); the monolayers were prepared using two different spreading solvents, chloroform and water, to examine the influence of spreading solvent on the properties of the monolayer. Chloroform is the standard solvent for preparation of Langmuir monolayers in laboratory studies; PLGA–PEG becomes molecularly dissolved in chloroform. In real therapeutic applications, however, chloroform cannot be used as the spreading solvent. The formulation must be water-based. The aqueous PLGA–PEG spreading solution was prepared using solvent exchange. In aqueous solution, PLGA–PEG exists in the form of micelles. As shown in the figure, unlike the chloroform-spread PLGA–PEG monolayer, the water-spread monolayer was unable to produce sufficiently high surface pressure (low surface tension); in the water-spread situation, the highest surface pressure observed was only about 25–30 mN/m at the highest compression level tested, which is insufficient to produce therapeutic effects.

The reason why the chloroform-spread versus water-spread PLGA–PEG monolayers exhibit drastically different surface tension isotherms is due to a difference in monolayer morphology. In the chloroform-spread monolayer system, the PLGA–PEG polymers form a molecularly spread (“anchor-brush”) monolayer.³² In the water-spread situation, the polymers remain in the micelle state even after being spread on the water surface. PLGA–PEG micelles are highly water-compatible.³² Thus, under high compression, PLGA–PEG micelles desorb from the air–water interface and submerge into the subphase thereby resisting to the compression (and thereby producing high surface pressure). We have been experimenting with water-spread monolayers prepared from various PLGA–PEG polymers having a range of different molecular weights (3.5–28.6 kg/mol) and PEG weight fractions (28.4–74.3%). None of these samples have been observed to be able to produce sufficiently high surface pressure; even under high compression, the surface pressure has never been seen to exceed about 30 mN/m. The details of this study have recently been reported in a separate publication.³²

To achieve high surface pressure, we decided to explore use of polymer micelles having stronger tendency to adsorb to the air–water interface. Specifically, we tested micelles formed by block copolymers containing more strongly hydrophobic segments such as PS–PEG micelles. Although they are both insoluble in water, PLGA and PS are very different in their levels of hydrophobicity. PS is far more hydrophobic than PLGA; PS has an interfacial tension with water of $\gamma_{\text{PS-water}} = 41$ mN/m, whereas PLGA has a much smaller interfacial tension with water ($\gamma_{\text{PLGA-water}} = 24.7$ mN/m). For this reason, PEG corona chains of PS–PEG micelles are expected to assume collapsed conformations to minimize the exposure of the hydrophobic PS domain to water; PS–PEG micelles are overall more hydrophobic and thus have a stronger affinity to the air–water interface than PLGA–PEG micelles (as a result, PS–PEG micelles are expected to give rise to higher surface pressures under compression). In the literature, collapsed micellar PEG brush structures have been documented for, for instance, poly(butadiene-*block*-ethylene glycol) (PB–PEG) micelles ($\gamma_{\text{PB-water}}$ of 45.9 mN/m).^{43,44} To confirm that PEG chains exist in a collapsed state, the mobility of the PEG brush segments of PS–PEG micelles were investigated by *in situ* NMR spin relaxation measurements; measurements were also performed in PLGA–PEG micelles for comparison. The longitudinal relaxation times (T_1) were measured by the inversion recovery method, and the transverse relaxation times (T_2) were measured using the Carr–Purcell–Meiboom–Gill (CPMG) spin echo sequence; T_1 is related to the chemical structure (“fast mode”), and T_2 is related to the configuration (“slow mode”) of the chain segment.⁴⁵

Between PS–PEG and PLGA–PEG micelles, it is expected that the PEG T_1 values are identical, whereas their T_2 values are significantly discrepant. NMR measurements were performed on four representative systems: PS(5610)–PEG(5000), PS(13832)–PEG(5000) and PLGA(4030)–PEG(5000) micelles, and PEG(5000) homopolymers in heavy water. For PS–PEG micelles, two separate PEG proton peaks were observed (a sharp (“hydrated PEG”) peak at ~ 3.61 ppm, and a broad (“collapsed PEG”) peak at ~ 3.56 ppm) (Figure 4a); the NMR spectra of PLGA–PEG micelles (and PEG homopolymers) exhibited only one sharp peak of hydrated PEG at ~ 3.63 ppm (Figure 4a). The 2D ^1H – ^{13}C

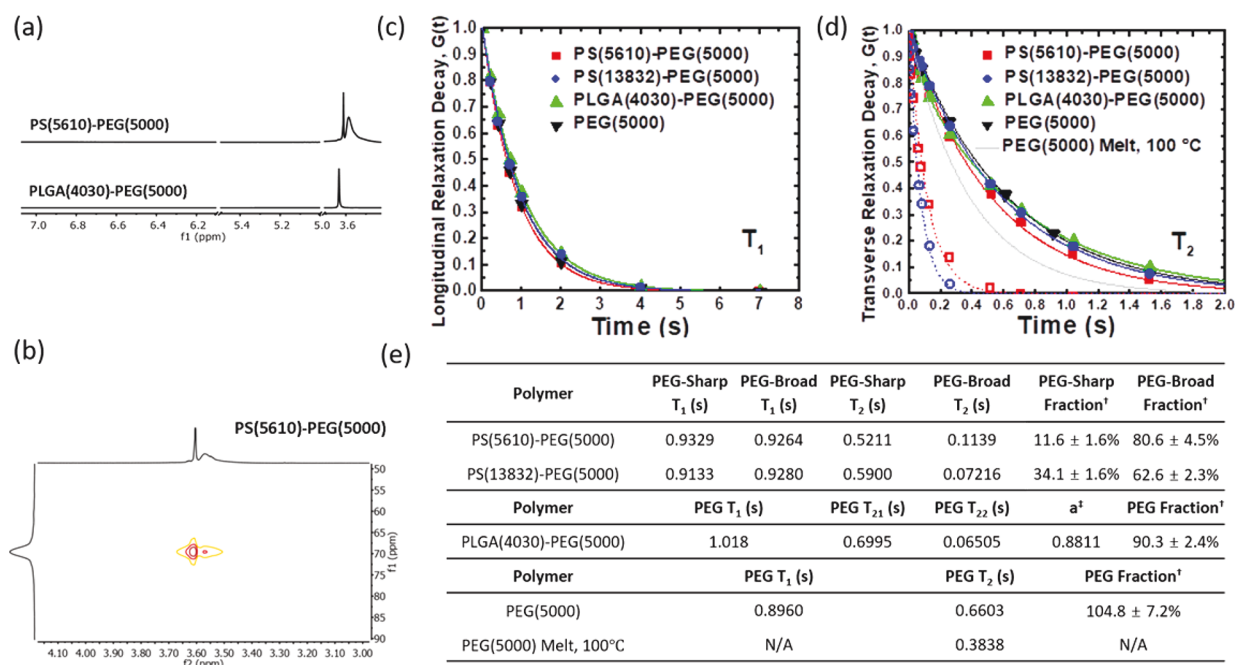


Figure 4. (a) 1D ^1H NMR Spectra for PS(5610)–PEG(5000) and PLGA(4030)–PEG(5000) in D_2O at 25 °C. (b) 2D ^1H – ^{13}C heteronuclear multiple bond correlation (HMBC) NMR spectra for PS(5610)–PEG(5000) in D_2O at 25 °C. (c) Longitudinal relaxation decay curves for PEG protons at 25 °C. Solid curves are fits to a mono-exponential decay function ($G(t) = \exp(-t/T_1)$). (d) Transverse relaxation decay curves for PEG protons at 25 °C. As demonstrated in panel a, spectra from PS(5610)–PEG(5000) and PS(13832)–PEG(5000) micelles exhibited two PEG peaks (a sharp peak at ~ 3.61 ppm and a broad peak at ~ 3.56 ppm). The decay curves of these peaks were separately fitted with a mono-exponential decay function. Open symbols represent broad PEG peaks, and filled symbols represent sharp PEG peaks. Spectra from PEG(5000) and PLGA(4030)–PEG(5000) exhibited single PEG peaks (also demonstrated in panel a). The decay curve of PEG(5000) was fit with the mono-exponential function, and that of PLGA(4030)–PEG(5000) was fit with a bi-exponential function ($G(t) = a \times \exp(-t/T_{21}) + (1 - a) \times \exp(-t/T_{22})$). (e) Best-fit T_1 and T_2 values. For all regressions the coefficient of determination (R^2) was greater than 0.99. Daggers indicate fractions of PEG segments contributing to the sharp and broad PEG peaks out of the total number of PEG segments available in the system, estimated based on pyridine internal reference. Double daggers indicate the coefficient of the first term of the biexponential decay function, a . Also shown for comparison is a predicted T_2 value for PEG(5000) melt at 100 °C (see the text for details).

heteronuclear multiple bond correlation (HMBC) NMR spectra (Figure 4b) confirmed that the two peaks in the PS–PEG spectra were not due to impurities. These two peaks were separately analyzed for T_1 and T_2 . The results are displayed in Figure 4c,d.

As shown in Figure 4c, all four samples, including PS(13832)–PEG(5000), PLGA(4030)–PEG(5000), and PEG(5000) exhibited a nearly identical PEG T_1 value (0.91 ± 0.03 s), which confirms the validity of the measurements. To the contrary, the measured PEG T_2 values varied significantly from sample to sample. To provide a scale of the PEG mobility, the T_2 value for 5 kg/mol PEG homopolymer melt at 100 °C was calculated; at this condition, PEG has a Rouse time of 281.52 ps, which translates to $T_2 = 0.3838$ s.⁴⁶ Hydrated PEG chains are expected to have longer T_2 values than 0.3838 s because of their higher mobility. The T_2 value for hydrated free PEG(5000) chains was estimated to be 0.6604 s from a fitting of the transverse decay curve to a monoexponential function, $G(t) = \exp(-t/T_2)$. The transverse decay curve of PLGA(4030)–PEG(5000) micelles was fit better with a biexponential function, $G(t) = a \times \exp(-t/T_{21}) + (1 - a) \times \exp(-t/T_{22})$ because the mobility of PEG segments vary depending on the proximity of the PEG segment to the grafting surface. T_{21} corresponded to PEG segments distant from the grafting surface, which were largely responsible for the overall signal intensity ($a = 0.8811$). T_{22} corresponded to PEG segments close to the grafting surface. The T_{21} value of PLGA–PEG micelles was higher than that of PEG melt and

slightly lower than that of hydrated PEG(5000), which indicates that the PEG corona chains of PLGA–PEG micelles were indeed fully hydrated.

For PS–PEG micelles, NMR spectra exhibited two separate PEG peaks (as demonstrated in Figure 4a). These two PEG peaks were separately fit with a mono-exponential function. The T_2 values obtained from the decay curves of the sharp PEG peaks of PS–PEG micelles were comparable to the T_{21} value obtained from PLGA–PEG micelles, which suggests that the sharp PEG peaks corresponds to the hydrated PEG segments of PS–PEG micelles. However, the T_2 values obtained from the broad PEG peaks of PS–PEG micelles were very small, even smaller than the T_2 value obtained from PEG melt, which unambiguously indicates that, in PS–PEG micelles, substantial portions of PEG segments existed in a collapsed state (because of the strong hydrophobicity of the PS material).

Further, it is very interesting to note that PS(13832)–PEG(5000) micelles has a higher fraction of hydrated PEG segments compared with PS(5610)–PEG(5000) micelles. The absolute concentrations of hydrated versus collapsed PEG segments of PS–PEG micelles could be determined using an NMR signal from pyridine added as an internal standard. PS(13832)–PEG(5000) micelles were found to have a significantly higher proportion of hydrated PEG segment ($34.1 \pm 1.6\%$) than PS(5610)–PEG(5000) micelles ($11.6 \pm 1.6\%$) (see the table at the bottom of Figure 4). As shown in Table S1, the degree of PEG brush hydration might have

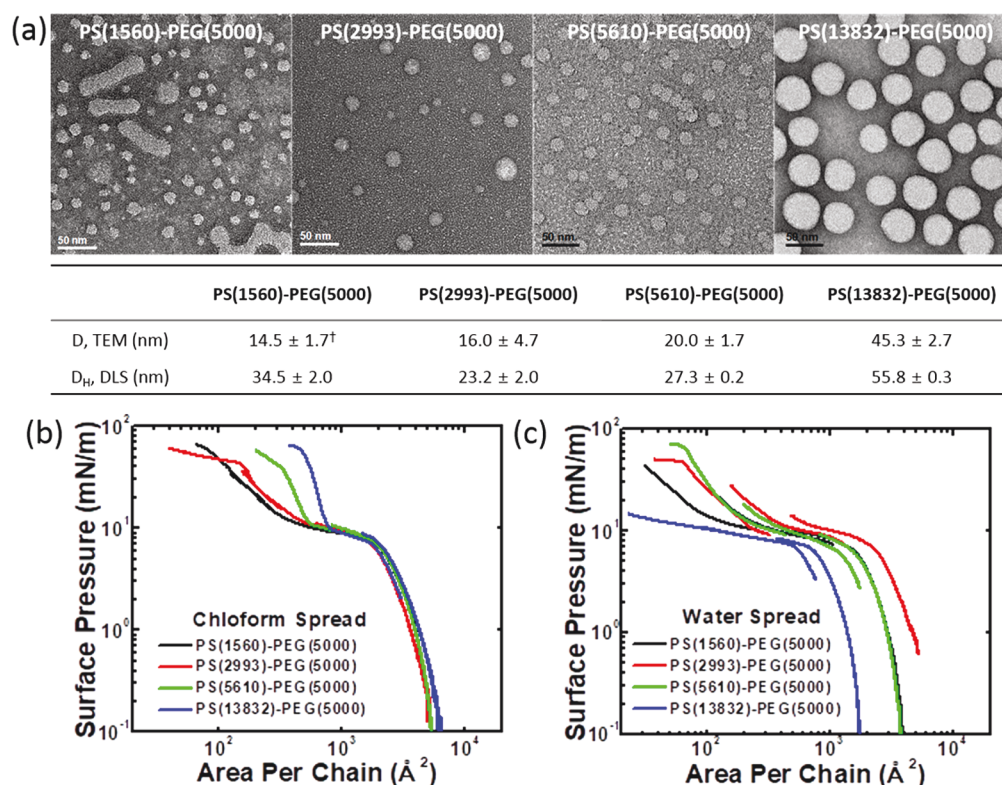


Figure 5. (a) TEM images of PS–PEG micelles formed in bulk water solutions. The dried micelle samples were negatively stained with uranyl acetate. Summarized in the table at the bottom are diameters of PS–PEG micelles as determined by TEM or DLS. Daggers indicate that they exclude elongated micelles. Molecular-packing properties of PS–PEG micelles (i.e., the micelle aggregation number, the interfacial area per chain, the dimensionless PEG grafting density, and the degree of PS chain stretching) estimated from the TEM data are summarized in Table S1. Constant-compression surface pressure–area isotherms of (b) chloroform-spread and (c) water-spread monolayers of 4 different PS–PEG materials at 25 °C. Milli-Q-purified water (18 MΩ·cm resistivity) was used as the subphase. In each panel, the isotherm curves from right to left were obtained, respectively, by initially spreading 4, 16, and 64 μL of 5 mg/mL PS–PEG solution in (b) chloroform or (c) water on the 780 cm² subphase surface. The subphase volume was 1.4 L. The monolayer compression rate was 3 mm/min.

connection with the degree of PS chain stretching and other properties of the PS core domain such as its glass transition temperature. The exact origin of the observed molecular weight trend is unclear at the present time. Further investigation is warranted. Nonetheless, these results clearly support that PS(13832)–PEG(5000) micelles are less hydrophobic (i.e., contain more hydrated PEG segments) than PS(5610)–PEG(5000) micelles and are therefore expected to be less strongly bound to the air–water interface.

In the literature, in fact, it has been documented that surface micelles formed by spreading a PS–PEG solution in chloroform onto the water surface typically exhibit high surface pressure (>60 mN/m) at high compression.^{47,48} Chloroform-spread PS–PEG surface micelles are anisotropic in molecular morphology because of the asymmetry of the air–water interface; in bulk water solution, isotropic (or axisymmetric, at least) micelle morphologies are typically obtained (Figure 5a). This morphological difference might produce a difference in the surface pressure–area isotherm. Prior to this investigation, it was unknown whether water-spread PS–PEG micelle monolayers would be able to produce similar high surface pressure as required for use in LS therapeutic applications. The surface pressure–area isotherms were measured for four different PS–PEG materials, PS(1560)–PEG(5000), PS(2993)–PEG(5000), PS(5610)–PEG(5000), and PS(13832)–PEG(5000) (both chloroform-spread and water-spread). The data are presented in Figure

5b,c. For constructing a full surface pressure–area isotherm curve over a large range of monolayer area, it was necessary to perform multiple (two or three) measurements in different ranges of monolayer area because of the size limitation of the Langmuir trough. Interestingly, the isotherms obtained from chloroform-spread monolayers over different areas superimposed closely on one another without breaking (Figure 5b), which suggests that when the polymers were spread from chloroform solutions, the loss of material to the subphase was negligible. However, as shown in Figure 5c, the curves from different areas for water-spread monolayers were disjointed, which suggests that the water-spreading procedure caused some loss of material (PS–PEG micelles) to the subphase. This trend is consistent with what was observed in experiments with PLGA–PEG (Figure 3).

Chloroform-spread PS–PEG monolayers exhibited similar isotherm profiles at surface pressures of <<10 mN/m regardless of the PS block molecular weight (Figure 5(b)). When compressed beyond the 10 mN/m surface pressure level, higher PS block molecular weights produced steeper rises in surface pressure for the chloroform-spread monolayers (Figure 5b). We suspect that this observation is due to the fact that higher molecular weight PS segments result in larger-sized core domains for the PS–PEG surface micelles.^{47,48} Unlike the chloroform-spread cases, the surface pressures of water-spread PS–PEG monolayers did not exhibit a monotonic trend with respect to the PS block molecular weight. One notable

observation was that in water-spread systems, maximum surface pressure was achieved at an intermediate PS block molecular weight; the steepest rise of surface pressure during compression was observed with the water-spread PS(5610)–PEG(5000) micelle monolayer (Figure 5c). Interestingly, the water-spread PS(13832)–PEG(5000) monolayer exhibited the lowest maximum surface pressure among all systems tested (Figure 5c). The maximum surface pressure of water-spread PS(13832)–PEG(5000) (10–20 mN/m) was comparable with those of water-spread PLGA–PEG micelles. These results are consistent with the above NMR results that water-spread PS(13832)–PEG(5000) micelles have a higher proportion of hydrated PEG segments ($34.1 \pm 1.6\%$) than water-spread PS(5610)–PEG(5000) micelles ($11.6 \pm 1.6\%$). These results suggest that appropriate values for molecular parameters (e.g., PS molecular weight relative to PEG molecular weight) should be chosen to satisfy the high-surface-pressure requirement for use in surfactant replacement therapy.

Overall, our investigation has now led to an identification of a promising class of candidate materials that have the desired surface tension and pressure properties for potential LS applications: e.g., the PS(5610)–PEG(5000) block copolymer formulated in the form of aqueous micelles. Aqueous micelle solutions of PS(5610)–PEG(5000) exhibit excellent colloidal stability over a long period of time; a PS(5610)–PEG(5000) micelle sample was confirmed to reproduce the same surface pressure–area profile after being stored at room temperature for at least 3 months.

Protein Resistance, Safety, and Efficacy. In ARDS, respiratory failure (atelectasis and de-recruitment of the alveoli) is aggravated due to deactivated LSs caused by an increased level of surface active deactivating agents such as serum proteins.^{22,49} Therapeutics developed for treatment of NRDS are not effective in treating adult ARDS, because of the deactivation of injected LSs.^{11,50} The protein resistance characteristics of PS(4418)–PEG(5000) micelle LSs were evaluated; during the course of this study, a shortage of the original PS(5610)–PEG(5000) sample was encountered, and a new batch of polymer (“PS(4418)–PEG(5000)”) was prepared that has a slightly lower PS block molecular weight and a slightly higher PDI (Figure 2). This PS(4418)–PEG(5000) material formed stable micelles of 47.3 ± 1.2 nm hydrodynamic diameter in water, and water-spread PS(4418)–PEG(5000) micelles were confirmed to produce high surface pressure (close to 70 mN/m) under high compression similar to PS(5610)–PEG(5000) micelles. A commercial LS, Infasurf (ONY), was used as the control; Infasurf has been known to have the highest therapeutic effect for NRDS treatment.^{51,52}

The main reason why current surfactant therapeutic formulations for NRDS (animal-extracted lipid–protein formulations such as Infasurf, Survanta, and Curosurf) are not effective in treating adult ARDS is the surfactant deactivation caused by deactivating agents (e.g., serum proteins).^{16,26} In this study, we first tested how Infasurf responds to an addition of a surface active protein, bovine serum albumin (BSA). As shown in Figure 6a, BSA deactivated Infasurf. Upon injection of BSA into the subphase of the Infasurf monolayer, Infasurf lost its capability to increase the surface pressure above 60 mN/m; the maximum surface pressure decreased (from about 65 mN/m) down to about 28 mN/m. BSA also has a similar effect on Survanta (data not

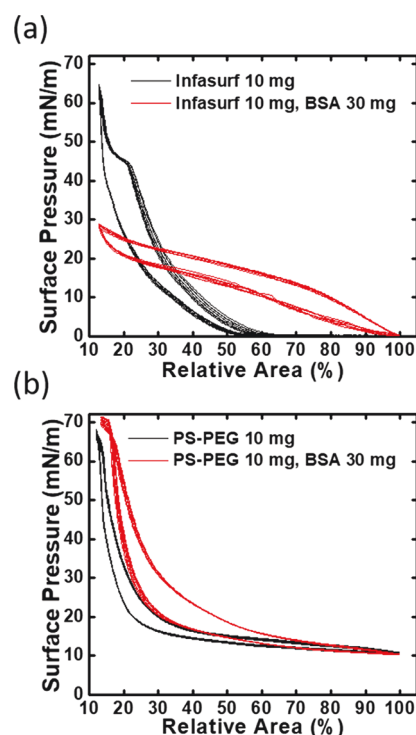


Figure 6. Surface pressure–area isotherms for (a) Infasurf (10 mg; 7.14 micrograms per milliliter of subphase) with and without the addition of BSA (30 mg; 21.4 micrograms per milliliter of subphase), and (b) water-spread PS(4418)–PEG(5000) (10 mg; 7.14 micrograms per milliliter of subphase) with and without the addition of BSA (30 mg; 21.4 micrograms per milliliter of subphase) during repeated compression–expansion cycles. A typical experiment was performed as follows: (1) Infasurf or PS(4418)–PEG(5000) was water-spread on water; (2) 30 min were waited for equilibration; (3) BSA was injected into the subphase without perturbing the Infasurf or PS(4418)–PEG(5000) interface; (4) compression–expansion cycles were initiated following a 10 min waiting period. The data displayed represent the last 10 compression–expansion cycles of a total 50 continuous cycles performed after spreading Infasurf or PS–PEG micelles. The subphase solution used contained 150 mM NaCl, 2 mM CaCl_2 , and 0.2 mM NaHCO_3 (pH 7.0–7.4, 25 °C). The monolayer was compressed and expanded at a rate of 50 mm/min; one compression–expansion cycle took 7.18 min. At the “100% relative area”, 10 mg of Infasurf or PS(4810)–PEG(5000) was spread on water in a Langmuir trough with 780 cm^2 surface area and 1.4 L subphase volume; “100% relative areas” corresponded to 0.972 and 12.2 square angstroms per molecule for Infasurf and PS(4418)–PEG(5000), respectively.

shown). To the contrary, the surface activity of PS–PEG micelles was largely unaffected by added BSA (Figure 6b).

The safety and efficacy of the PS(4418)–PEG(5000) micelle LS were evaluated *in vivo* in C57/BL6 mice (8–12 weeks old, female). The PS(4418)–PEG(5000) micelle solution became highly viscous (i.e., non-Newtonian) at polymer concentrations greater than about 6 wt % (60 mg/mL). A maximum tolerated dose (MTD) study was performed. In this MTD study, the effects of three PS(4418)–PEG(5000) dose levels (2.4, 24, and 240 milligrams of polymer per kilogram of mouse body weight) were studied ($N = 1$); fixed volumes of polymer solutions (4 milliliters per kilogram of mouse body weight) at 3 different polymer concentrations (0.6, 6, and 60 mg/mL) were administered into mice via nonsurgical intratracheal instillation (4 mL/kg represents the

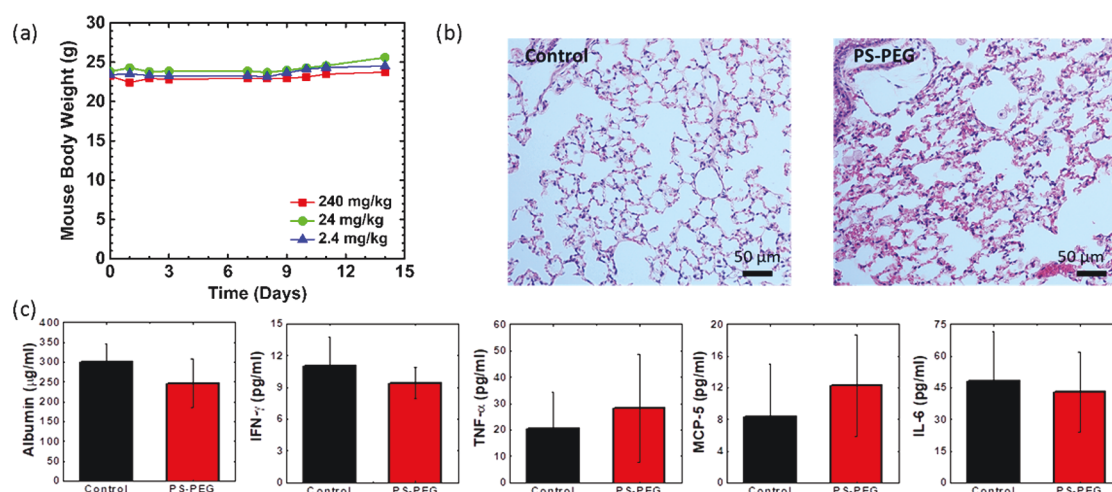


Figure 7. (a) Mouse body weights recorded as a function of time following intratracheal instillation of different doses of PS(4418)–PEG(5000) micelles at day 0 ($N = 1$). (b) A representative H&E-stained histological section of the lungs taken at 7 days after intratracheal injection of 240 mg PS(4418)–PEG(5000) micelles per kilogram of body weight in mice ($N = 1$). (c) Levels of albumin and 4 different cytokines in BAL fluids collected from mice at 7 days after intratracheal injection of 240 mg/kg PS(4418)–PEG(5000) micelles. BAL fluids from untreated mice were used as control. Measurements were performed in quadruplicate ($N = 4$). Error bars represent standard deviations. The assessment of statistical significance is summarized in Table S2.

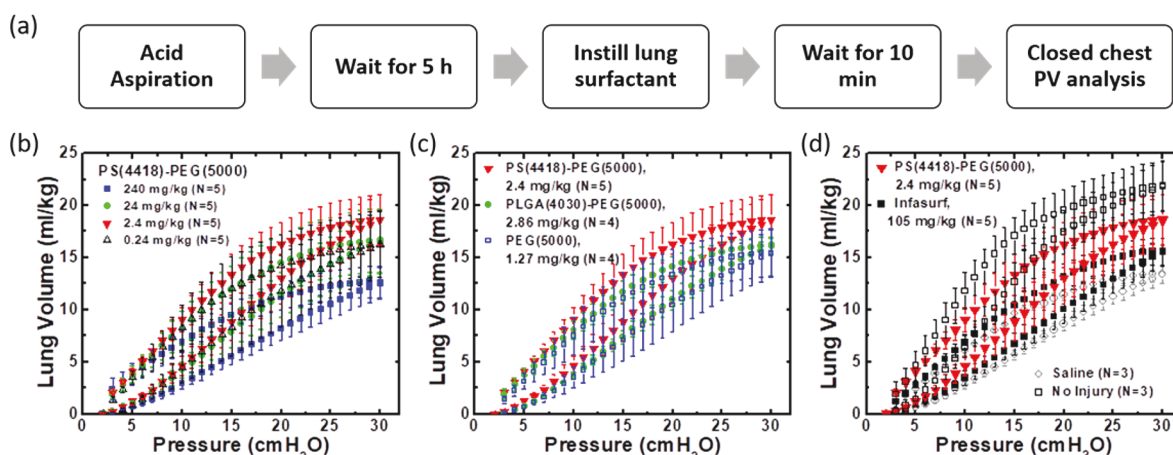


Figure 8. (a) Diagrammatic description of the procedures used in LS efficacy tests using acid aspiration lung injury ARDS mouse models. (b) Closed-chest pressure–volume (PV) curves of acid-injured mouse lungs following intratracheal instillation of PS(4418)–PEG(5000) micelles at four different polymer doses. (c) Closed-chest PV curves of acid-injured mouse lungs following intratracheal instillation of PS(4418)–PEG(5000) micelles (0.600 mg/mL \times 4.0 mL/kg), PLGA(4030)–PEG(5000) micelles (0.714 mg/mL \times 4.0 mL/kg) or PEG(5000) homopolymers (0.3185 mg/mL \times 4.0 mL/kg). (d) Closed-chest PV curves of acid-injured mouse lungs following intratracheal instillation of PS(4418)–PEG(5000) (0.600 mg/mL \times 4.0 mL/kg), Infasurf (35.0 mg/mL \times 3.0 mL/kg), or saline (4.0 mL/kg). Also included is the curve from noninjured mice (“No Injury”). Error bars represent standard deviations (N values shown in legends). The assessment of statistical significance is summarized in Table S3.

maximum tolerated volume for an intratracheal injection of a liquid that does not cause injury or blockage in the lungs of a mouse). Following polymer instillation, mice were monitored for symptoms of toxicity (weight loss and behavior change such as abnormal responses to light, sound and motion, and breathing irregularity) for 14 days. The body-weight profiles are presented in Figure 7a. At all dose levels, no signs of toxicity were observed for the 14 day period. The MTD of PS(4418)–PEG(5000) micelles is greater than 240 mg/kg. Further dose escalation was not attempted because 240 mg/kg already far exceeds the therapeutic dose (as will be discussed later).

Toxicological analysis was performed on the lungs of mice instilled with PS(4418)–PEG(5000) micelles at the 240 mg/kg dose level; lung histology slides ($N = 1$) and bronchoalveolar lavage (BAL) fluids ($N = 4$) were collected

at 7 days after injection. A representative H&E-stained histological section of the lungs is presented in Figure 7b. No histopathological changes were detected in the lungs treated with PS(4418)–PEG(5000) micelles relative to the untreated control. BAL fluids were analyzed for levels of albumin (to detect permeability injury) and cytokines that reflect inflammation (IFN- γ , TNF- α , MCP-5, and IL-6). The results are presented in Figure 7c. As shown in the figure, the levels of these five markers were not significantly different between baseline assessment and 240 mg/kg PS(4418)–PEG(5000) treatment, confirming the safety of this treatment; see Table S2 for statistical analysis of the data shown in Figure 7c.

The efficacies of polymer LSs were tested in a mouse model of acid aspiration-induced lung injury. Quasi-static closed-chest pressure–volume (PV) measurements were used to determine

the level of lung injury. Figure 8a presents a schematic representation of the overall test procedure. The deactivation of LS due to lung injury causes a downward shift of the PV relationship (because of the reduced compliance of the lungs), whereas a successful treatment with therapeutic LS would shift the PV curve upward (because of the recovered compliance of the lungs). In Figure 8d, reference PV curves for both healthy and acid-injured mouse lungs are displayed (marked as “No Injury” and “Saline (No Treatment)”, respectively, in the figure); in other figures (Figure 8b,c) these “No Injury” and “Saline” curves are omitted for clarity. Treatment efficacy is gauged by how much the PV curve is shifted upward from the acid-injured state (“Saline”) to the recovered healthy state (“No Injury”) upon treatment. First, to determine the optimal therapeutic dose for PS(4418)–PEG(5000), closed-chest PV tests were performed at four different polymer doses: 0.24, 2.4, 24, and 240 milligrams of polymer per kilogram of body weight. As shown in Figure 8b, the highest efficacy (the greatest upward shift of the PV curve) was obtained at 2.4 mg PS(4418)–PEG(5000)/kg. This optimal dose value is quite consistent with the theoretical amount of surfactant material needed to coat the whole surface area of the lungs (~ 3.1 mg/kg),²⁷ which supports that PS(4418)–PEG(5000) micelles indeed form an insoluble monolayer at the alveolar air–water interface. At lower doses, polymer’s efficacy is lower because the absolute amount of polymer available is insufficient to cover the whole air–water interface. However, the lower efficacy seen at higher polymer doses was unexpected; it appears that higher doses of PS(4418)–PEG(5000) produced adverse biological effects in acid-injured lungs. The exact origin of this behavior requires further study.

To validate whether the efficacy of PS(4418)–PEG(5000) micelles indeed originates from their strong tendency adsorb to the air–water interface, quasi-static closed-chest PV tests were also performed on less-surface-active compounds, PLGA(4030)–PEG(5000) micelles and PEG(5000) homopolymers; water-spread PLGA–PEG micelles and PEG homopolymers are normally unable to produce high surface pressure because they are prone to desorb from the air–water interface under high compression. For comparison with PS(4418)–PEG(5000) micelles at 2.4 mg/kg, a dose level of 2.86 mg/kg was used for PLGA(4030)–PEG(5000) micelles, and a dose level of 1.27 mg/kg for PEG(5000) homopolymers, which gave the same PEG dose value (1.27 mg/kg) for all three systems. The results displayed in Figure 8c strongly support that in vivo therapeutic efficacy clearly correlates with high surface pressure generating capability.

To demonstrate the role of protein resistance in producing efficacy in treating ARDS, Figure 8d compares closed-chest PV curves for protein-resistant PS(4418)–PEG(5000) micelles and a protein-deactivatable commercial NRDS LS, Infasurf; see Figure 6 for effects of serum proteins on the air–water interfacial activities of these compounds. For Infasurf, closed-chest PV tests were performed using a dose level of 105 mg/kg (35 mg/mL concentration \times 3 mL/kg dose volume). In previous clinical testing of Infasurf in adult ARDS patients, an insufficient dose ($= 60$ mg/mL \times 1 mL/kg) has been used; the study failed to demonstrate therapeutic benefits.¹³ In a different clinical trial involving pediatric ARDS patients, a higher Infasurf dose ($= 35$ mg/mL \times 3 mL/kg) was tested, which resulted in an improved treatment outcome;⁵³ the lungs of adult mice are known to be physiologically closer to the lungs of pediatric patients than those of adults.² For this

reason, we chose the 105 mg/kg dose for Infasurf. As shown in Figure 8d, protein-resistant PS(4418)–PEG(5000) micelles indeed produce greater recovery of acid-injured lungs than protein-sensitive Infasurf. It should be noted that the dose level used for PS(4418)–PEG(5000) micelles was equal to only about 2.3% of that used for Infasurf. In a previous clinical trial testing aerosolized Exosurf for treatment of ARDS, the unsuccessful outcome has been attributed to low efficiency of delivery; only less than 4.5% of injected dose (< 5 mg out of 112 mg aerosolized DPPC per kg per day) reached the deep lungs.⁵⁴ The significantly lower amount of polymer needed to produce therapeutic effect might serve as an enabling factor for aerosol delivery of the formulation to the lung.

Our data suggest that polymer LSs have great potential for use in ARDS therapy. Since the initial development of animal-derived NRDS therapeutics in the 1980s, little further progress has been achieved in this field. Aerosol delivery and synthetic protein replacement have been the main thrust in research, but efforts have been met with limited success.^{55–58} Testing fully synthetic polymer materials for ARDS and NRDS treatments represents a radical shift in the direction of LS research. Polymer LSs may open the door to new therapeutic options for the treatment of ARDS that had not previously been feasible with conventional lipid-based NRDS therapeutics.

4. CONCLUSIONS

For the first time, the concept of using a completely synthetic polymer material as an active ingredient in ARDS and NRDS therapeutics is proposed, and its safety and feasibility has been demonstrated. Polymer LS has the potential to address the limitations of current animal-derived lipid-based NRDS therapeutics: high production and treatment costs, limited supply, and complex delivery procedures. Polymer LSs have far longer shelf lives and would not require any complicated pretreatment processes prior to use in treatment. Unlike lipid-based LSs, the dynamic surface active characteristics of polymer LSs do not degrade even in the presence of competing surface active proteins. In preliminary animal studies, it was confirmed that intratracheally administered polymer LSs can be tolerated without causing damage to the lungs in mice and are capable of producing dose-dependent effects on improving the compliance of acid-injured mouse lungs in vivo. Further research is warranted to optimize the formulation for maximum therapeutic effect and to evaluate the detailed short- and long-term toxicology and pharmacokinetics of the material.

■ ASSOCIATED CONTENT

Supporting Information

The Supporting Information is available free of charge on the ACS Publications website at DOI: 10.1021/acsabm.8b00061.

Tables showing the molecular-packing properties of PS–PEG micelles and statistical analysis of data presented in Figures 7 and 8 (PDF)

■ AUTHOR INFORMATION

Corresponding Author

*E-mail: yywon@ecn.purdue.edu.

ORCID

You-Yeon Won: 0000-0002-8347-6375

Notes

The authors declare the following competing financial interest(s): A company, Spirrow Therapeutics, is currently attempting to commercialize the technology discussed in this manuscript. H.K.K., D.Q.A., and Y.Y.W. have an ownership interest in this company.

ACKNOWLEDGMENTS

Funding for this research was provided by the NSF (grant nos. CBET-1264336 and IIP-1713953) and the NIH (grant no. NIGMS R01 GM111305-01). We also thank Mr. Scott Verner at ONY for generously providing us with Infasurf and Prof. Robert Hannemann in the School of Chemical Engineering at Purdue University for assistance with the purchase of Survanta. We also wish to acknowledge support from the Purdue University Center for Cancer Research (PCCR) via an NIH NCI grant (P30 CA023168), which supports the campus-wide NMR shared resources that were utilized in this work.

REFERENCES

- (1) Farrell, P. M.; Wood, R. E. Epidemiology of Hyaline Membrane Disease in the United States: Analysis of National Mortality Statistics. *Pediatrics* **1976**, *58* (2), 167–176.
- (2) Hogan, B. L. M.; Barkauskas, C. E.; Chapman, H. A.; Epstein, J. A.; Jain, R.; Hsia, C. C. W.; Niklason, L.; Calle, E.; Le, A.; Randell, S. H.; Rock, J.; Snitow, M.; Krummel, M.; Stripp, B. R.; Vu, T.; White, E. S.; Whitsett, J. A.; Morrissey, E. E. Repair and Regeneration of the Respiratory System: Complexity, Plasticity, and Mechanisms of Lung Stem Cell Function. *Cell Stem Cell* **2014**, *15* (2), 123–138.
- (3) Notter, R. H. *Lung Surfactants: Basic Science and Clinical Applications*; Taylor & Francis: Abingdon, United Kingdom, 2000.
- (4) Wrobel, S. Bubbles, Babies and Biology: The Story of Surfactant. *FASEB J.* **2004**, *18* (13), 1624e.
- (5) Singh, G. K.; van Dyck, P. C. *Infant Mortality in the United States, 1935–2007. Over Seven Decades of Progress and Disparities*; U.S. Department of Health and Human Services, Health Resources and Services Administration, Maternal and Child Health Bureau: Washington, DC, 2010.
- (6) Barber, M.; Blaisdell, C. J. Respiratory Causes of Infant Mortality: Progress and Challenges. *Amer J. Perinatol* **2010**, *27* (07), 549–558.
- (7) Hudson, L. D.; Milberg, J. A.; Anardi, D.; Maunder, R. J. Clinical Risks for Development of the Acute Respiratory Distress Syndrome. *Am. J. Respir. Crit. Care Med.* **1995**, *151* (2), 293–301.
- (8) Nathens, A. B.; Jurkovich, G. J.; MacKenzie, E. J.; Rivara, F. P. A Resource-Based Assessment of Trauma Care in the United States. *J. Trauma* **2004**, *56* (1), 173–178.
- (9) Angus, D. C.; Linde-Zwirble, W. T.; Lidicker, J.; Clermont, G.; Carcillo, J.; Pinsky, M. R. Epidemiology of Severe Sepsis in the United States: Analysis of Incidence, Outcome, and Associated Costs of Care. *Crit. Care Med.* **2001**, *29* (7), 1303–1310.
- (10) Ranieri, V. M.; Rubenfeld, G. D.; Thompson, B. T.; Ferguson, N. D.; Caldwell, E.; Fan, E.; Camporota, L.; Slutsky, A. S. Acute Respiratory Distress Syndrome: the Berlin Definition. *JAMA* **2012**, *307* (23), 2526–2533.
- (11) Spragg, R. G.; Lewis, J. F.; Walrath, H.-D.; Johannigman, J.; Bellingan, G.; Laterre, P.-F.; Witte, M. C.; Richards, G. A.; Rippin, G.; Rathgeb, F.; Häfner, D.; Taut, F. J. H.; Seeger, W. Effect of Recombinant Surfactant Protein C–Based Surfactant on the Acute Respiratory Distress Syndrome. *N. Engl. J. Med.* **2004**, *351* (9), 884–892.
- (12) Spragg, R. G.; Taut, F. J.; Lewis, J. F.; Schenk, P.; Ruppert, C.; Dean, N.; Krell, K.; Karabinis, A.; Gunther, A. Recombinant Surfactant Protein C–Based Surfactant for Patients with Severe Direct Lung Injury. *Am. J. Respir. Crit. Care Med.* **2011**, *183* (8), 1055–1061.
- (13) Willson, D. F.; Truitt, J. D.; Conaway, M. R.; Traul, C. S.; Egan, E. E. The Adult Calfactant in Acute Respiratory Distress Syndrome Trial. *Chest* **2015**, *148* (2), 356–364.
- (14) Kesecioglu, J.; Beale, R.; Stewart, T. E.; Findlay, G. P.; Rouby, J.-J.; Holzapfel, L.; Bruins, P.; Steenken, E. J.; Jeppesen, O. K.; Lachmann, B. Exogenous Natural Surfactant for Treatment of Acute Lung Injury and the Acute Respiratory Distress Syndrome. *Am. J. Respir. Crit. Care Med.* **2009**, *180* (10), 989–994.
- (15) Willson, D. F.; Thomas, N. J. Surfactant Composition and Biophysical Properties Are Important in Clinical Studies. *Am. J. Respir. Crit. Care Med.* **2010**, *181* (7), 762–762.
- (16) Seeger, W.; Grube, C.; Gunther, A.; Schmidt, R. Surfactant Inhibition by Plasma Proteins: Differential Sensitivity of Various Surfactant Preparations. *Eur. Respir. J.* **1993**, *6* (7), 971–977.
- (17) Filoche, M.; Tai, C.-F.; Grotberg, J. B. Three-Dimensional Model of Surfactant Replacement Therapy. *Proc. Natl. Acad. Sci. U. S. A.* **2015**, *112* (30), 9287–9292.
- (18) Grotberg, J. B.; Filoche, M.; Willson, D. F.; Raghavendran, K.; Notter, R. H. Did Reduced Alveolar Delivery of Surfactant Contribute to Negative Results in Adults with Acute Respiratory Distress Syndrome? *Am. J. Respir. Crit. Care Med.* **2017**, *195* (4), 538–540.
- (19) Kim, H. C.; Won, Y. Y. Clinical, technological, and economic issues associated with developing new lung surfactant therapeutics. *Biotechnol. Adv.* **2018**, *36* (4), 1185–1193.
- (20) Neumann, A. W.; David, R.; Zuo, Y. *Applied Surface Thermodynamics*, 2nd ed.; CRC Press: Boca Raton, FL, 2010.
- (21) Weaver, T. E.; Conkright, J. J. Function of Surfactant Proteins B and C. *Annu. Rev. Physiol.* **2001**, *63* (1), 555–578.
- (22) Spragg, R. G. Abnormalities of the Lung Surfactant System in Acute Lung Injury. In *Pathophysiology of Shock, Sepsis, and Organ Failure*; Schlag, G.; Redl, H., Eds.; Springer Berlin Heidelberg: Berlin, Heidelberg, 1993; pp 747–756.
- (23) Dohm, M. T.; Mowery, B. P.; Czyzewski, A. M.; Stahl, S. S.; Gellman, S. H.; Barron, A. E. Biophysical Mimicry of Lung Surfactant Protein B by Random Nylon-3 Copolymers. *J. Am. Chem. Soc.* **2010**, *132* (23), 7957–7967.
- (24) Kobayashi, T.; Ohta, K.; Tashiro, K.; Nishizuka, K.; Chen, W.-M.; Ohmura, S.; Yamamoto, K. Dextran restores albumin-inhibited surface activity of pulmonary surfactant extract. *J. Appl. Physiol.* **1999**, *86* (6), 1778–1784.
- (25) TAEUSCH, H. W.; LU, K. W.; GOERKE, J.; CLEMENTS, J. A. Nonionic Polymers Reverse Inactivation of Surfactant by Meconium and Other Substances. *Am. J. Respir. Crit. Care Med.* **1999**, *159* (5), 1391–1395.
- (26) Stenger, P. C.; Zasadzinski, J. A. Enhanced Surfactant Adsorption via Polymer Depletion Forces: A Simple Model for Reversing Surfactant Inhibition in Acute Respiratory Distress Syndrome. *Biophys. J.* **2007**, *92* (1), 3–9.
- (27) Marks, L. B.; Notter, R. H.; Oberdorster, G.; McBride, J. T. Ultrasonic and Jet Aerosolization of Phospholipids and the Effects on Surface Activity. *Pediatr. Res.* **1983**, *17* (9), 742–747.
- (28) Willson, D. F. Aerosolized Surfactants, Anti-Inflammatory Drugs, and Analgesics. *Respir Care* **2015**, *60* (6), 774–793.
- (29) Windtree announces top-line results from Aerosurf phase 2b clinical trial. **2017.20174**
- (30) Park, H.-W.; Choi, J.; Ohn, K.; Lee, H.; Kim, J. W.; Won, Y.-Y. Study of the Air–Water Interfacial Properties of Biodegradable Polyesters and Their Block Copolymers with Poly(ethylene glycol). *Langmuir* **2012**, *28* (31), 11555–11566.
- (31) Kim, H. C.; Lee, H.; Khetan, J.; Won, Y.-Y. Surface Mechanical and Rheological Behaviors of Biocompatible Poly ((D, L-lactic acid-ran-glycolic acid)-block-ethylene glycol)(PLGA-PEG) and Poly ((D, L-lactic acid-ran-glycolic acid-ran-ε-caprolactone)-block-ethylene glycol)(PLGACL-PEG) Block Copolymers at the Air–Water Interface. *Langmuir* **2015**, *31* (51), 13821–13833.
- (32) Kim, H. C.; Arick, D. Q.; Won, Y.-Y. Air–Water Interfacial Properties of Chloroform-Spread versus Water-Spread Poly((d,l-lactic acid-co-glycolic acid)-block-ethylene glycol) (PLGA-PEG) Polymers. *Langmuir* **2018**, *34* (16), 4874–4887.

- (33) Neises, B.; Steglich, W. Simple Method for the Esterification of Carboxylic Acids. *Angew. Chem., Int. Ed. Engl.* **1978**, *17* (7), 522–524.
- (34) Machado-Aranda, D.; Wang, Z.; Yu, B.; Suresh, M. V.; Notter, R. H.; Raghavendran, K. Increased Phospholipase A(2) and Lyso-Phosphatidylcholine Levels Are Associated with Surfactant Dysfunction in Lung Contusion Injury in Mice. *Surgery* **2013**, *153* (1), 25–35.
- (35) Dunn, S. E.; Brindley, A.; Davis, S. S.; Davies, M. C.; Illum, L. Polystyrene-Poly(ethylene glycol) (PS-PEG2000) Particles as Model Systems for Site Specific Drug Delivery. 2. The Effect of PEG Surface Density on the In Vitro Cell Interaction and In Vivo Biodistribution. *Pharm. Res.* **1994**, *11* (7), 1016–1022.
- (36) Kutscher, H. L.; Chao, P.; Deshmukh, M.; Sundara Rajan, S.; Singh, Y.; Hu, P.; Joseph, L. B.; Stein, S.; Laskin, D. L.; Sinko, P. J. Enhanced Passive Pulmonary Targeting and Retention of PEGylated Rigid Microparticles in Rats. *Int. J. Pharm.* **2010**, *402* (1–2), 64–71.
- (37) Beroström, K.; Österberg, E.; Holmberg, K.; Hoffman, A. S.; Schuman, T. P.; Kozłowski, A.; Harris, J. M. Effects of Branching and Molecular Weight of Surface-Bound Poly(ethylene oxide) on Protein Rejection. *J. Biomater. Sci., Polym. Ed.* **1995**, *6* (2), 123–132.
- (38) Meng, F.; Engbers, G. H. M.; Gessner, A.; Müller, R. H.; Feijen, J. Pegylated Polystyrene Particles as a Model System for Artificial Cells. *J. Biomed. Mater. Res., Part A* **2004**, *70A* (1), 97–106.
- (39) Laan, A. C.; Santini, C.; Jennings, L.; de Jong, M.; Bernsen, M. R.; Denkova, A. G. Radiolabeling Polymeric Micelles for In Vivo Evaluation: A Novel, Fast, and Facile Method. *EJNMMI Res.* **2016**, *6*, 12.
- (40) Zhang, L.; Eisenberg, A. Multiple Morphologies of “Crew-Cut” Aggregates of Polystyrene-*b*-Poly(acrylic acid) Block Copolymers. *Science* **1995**, *268*, 1728.
- (41) Zhang, L.; Eisenberg, A. Multiple Morphologies and Characteristics of “Crew-Cut” Micelle-like Aggregates of Polystyrene-*b*-poly(acrylic acid) Diblock Copolymers in Aqueous Solutions. *J. Am. Chem. Soc.* **1996**, *118* (13), 3168–3181.
- (42) Kim, H. C.; Lee, H.; Jung, H.; Choi, Y. H.; Meron, M.; Lin, B.; Bang, J.; Won, Y.-Y. Humidity-Dependent Compression-Induced Glass Transition of the Air-Water Interfacial Langmuir Films of Poly(D, L-lactic acid-*ran*-glycolic acid)(PLGA). *Soft Matter* **2015**, *11*, 5666–5677.
- (43) Won, Y.-Y.; Davis, H. T.; Bates, F. S.; Agamalian, M.; Wignall, G. D. Segment Distribution of the Micellar Brushes of Poly(ethylene oxide) via Small-Angle Neutron Scattering. *J. Phys. Chem. B* **2000**, *104* (30), 7134–7143.
- (44) Zheng, Y.; Won, Y.-Y.; Bates, F. S.; Davis, H. T.; Scriven, L. E.; Talmon, Y. Directly Resolved Core-Corona Structure of Block Copolymer Micelles by Cryo-Transmission Electron Microscopy. *J. Phys. Chem. B* **1999**, *103* (47), 10331–10334.
- (45) Levitt, M. H. *Spin Dynamics: Basics of Nuclear Magnetic Resonance*; Wiley: New York, 2001.
- (46) Ries, M. E.; Klein, P. G.; Brereton, M. G.; Ward, I. M. Proton NMR Study of Rouse Dynamics and Ideal Glass Transition Temperature of Poly(ethylene oxide) LiCF₃SO₃ Complexes. *Macromolecules* **1998**, *31* (15), 4950–4956.
- (47) Gonçalves da Silva, A. M.; Filipe, E. J. M.; d'Oliveira, J. M. R.; Martinho, J. M. G. Interfacial Behavior of Poly(styrene)-Poly(ethylene oxide) Diblock Copolymer Monolayers at the Air–Water Interface. Hydrophilic Block Chain Length and Temperature Influence. *Langmuir* **1996**, *12* (26), 6547–6553.
- (48) Gonçalves da Silva, A. M.; Simões Gamboa, A. L.; Martinho, J. M. G. Aggregation of Poly(styrene)-Poly(ethylene oxide) Diblock Copolymer Monolayers at the Air–Water Interface. *Langmuir* **1998**, *14* (18), 5327–5330.
- (49) Nakos, G.; Kitsioulis, E. I.; Tsangaris, I.; Lekka, M. E. Bronchoalveolar Lavage Fluid Characteristics of Early Intermediate and Late Phases of ARDS. *Intensive Care Med.* **1998**, *24* (4), 296–303.
- (50) Gregory, T. J.; Steinberg, K. P.; Spragg, R.; Gadek, J. E.; Hyers, T. M.; Longmore, W. J.; Moxley, M. A.; Cai, G. Z.; Hite, R. D.; Smith, R. M.; Hudson, L. D.; Crim, C.; Newton, P.; Mitchell, B. R.; Gold, A. J. Bovine Surfactant Therapy for Patients with Acute Respiratory Distress Syndrome. *Am. J. Respir. Crit. Care Med.* **1997**, *155* (4), 1309–1315.
- (51) Bloom, B. T.; Kattwinkel, J.; Hall, R. T.; Delmore, P. M.; Egan, E. A.; Trout, J. R.; Malloy, M. H.; Brown, D. R.; Holzman, I. R.; Coghill, C. H.; Carlo, W. A.; Pramanik, A. K.; McCaffree, M. A.; Toubas, P. L.; Laudert, S.; Gratny, L. L.; Weatherstone, K. B.; Seguin, J. H.; Willett, L. D.; Gutcher, G. R.; Mueller, D. H.; Topper, W. H. Comparison of Infasurf (Calf Lung Surfactant Extract) to Survanta (Beractant) in the Treatment and Prevention of Respiratory Distress Syndrome. *Pediatrics* **1997**, *100* (1), 31–38.
- (52) Attar, M. A.; Becker, M. A.; Dechert, R. E.; Donn, S. M. Immediate Changes in Lung Compliance Following Natural Surfactant Administration in Premature Infants with Respiratory Distress Syndrome: a Controlled Trial. *J. Perinatol.* **2004**, *24* (10), 626–630.
- (53) Willson, D. F.; Zaritsky, A.; Bauman, L. A.; Dockery, K.; James, R. L.; Conrad, D.; Craft, H.; Novotny, W. E.; Egan, E. A.; Dalton, H. Instillation of Calf Lung Surfactant Extract (Calfactant) Is Beneficial in Pediatric Acute Hypoxemic Respiratory Failure. *Crit. Care Med.* **1999**, *27* (1), 188–195.
- (54) Anzueto, A.; Baughman, R. P.; Guntupalli, K. K.; Weg, J. G.; Wiedemann, H. P.; Raventos, A. A.; Lemaire, F.; Long, W.; Zaccardelli, D. S.; Pattishall, E. N. Aerosolized Surfactant in Adults with Sepsis-Induced Acute Respiratory Distress Syndrome. Exosurf Acute Respiratory Distress Syndrome Sepsis Study Group. *N. Engl. J. Med.* **1996**, *334* (22), 1417–1421.
- (55) Berggren, E.; Liljedahl, M.; Winblad, B.; Andreasson, B.; Curstedt, T.; Robertson, B.; Schollin, J. Pilot Study of Nebulized Surfactant Therapy for Neonatal Respiratory Distress Syndrome. *Acta Paediatr.* **2000**, *89* (4), 460–464.
- (56) Lewis, J. F.; Ikegami, M.; Jobe, A. H.; Tabor, B. Aerosolized Surfactant Treatment of Preterm Lambs. *J. Appl. Physiol.* **1991**, *70* (2), 869–876.
- (57) Ellyett, K. M.; Broadbent, R. S.; Fawcett, E. R.; Campbell, A. J. Surfactant Aerosol Treatment of Respiratory Distress Syndrome in the Spontaneously Breathing Premature Rabbit. *Pediatr. Res.* **1996**, *39* (6), 953–957.
- (58) Dijk, P. H.; Heikamp, A.; Oetomo, S. B. Surfactant Nebulization versus Instillation during High Frequency Ventilation in Surfactant-Deficient Rabbits. *Pediatr. Res.* **1998**, *44* (5), 699–704.